



# A polymerized vinylene carbonate anode binder enhances performance of lithium-ion batteries

Hui Zhao<sup>a</sup>, Xin Zhou<sup>b</sup>, Sang-Jae Park<sup>a</sup>, Feifei Shi<sup>a</sup>, Yanbao Fu<sup>a</sup>, Min Ling<sup>a</sup>, Neslihan Yuca<sup>a</sup>, Vincent Battaglia<sup>a</sup>, Gao Liu<sup>a,\*</sup>

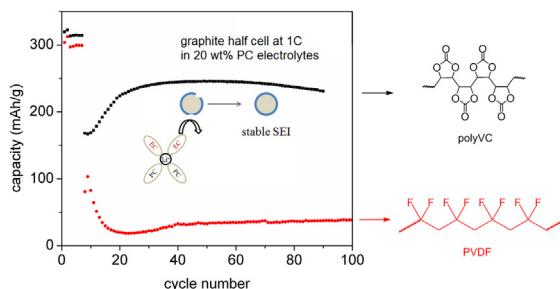
<sup>a</sup> Lawrence Berkeley National Laboratory, Berkeley, CA 94720, USA

<sup>b</sup> University of California, Los Angeles, CA 90095, USA

## HIGHLIGHTS

- A polymerized vinylene carbonate (polyVC) is used as binder.
- PolyVC shows better cell performance than PVDF.
- PolyVC promotes the formation of stable SEI.
- Propylene carbonate is successfully used in polyVC-based cell.

## GRAPHICAL ABSTRACT



## ARTICLE INFO

### Article history:

Received 8 February 2014

Received in revised form

12 April 2014

Accepted 14 April 2014

Available online 24 April 2014

### Keywords:

Vinylene carbonate

Graphite exfoliation

Lithium-ion battery

Solid electrolyte interphase (SEI)

## ABSTRACT

We investigated the use of polymerized vinylene carbonate (polyVC) as a binder for graphite anodes in lithium-ion cells. It functions not only of a traditional binder, but also plays an important role in surface stabilization of graphite in propylene carbonate (PC)-based electrolytes. In an electrolyte with PC content as high as 30 wt%, the polyVC binder enhanced battery performance, with a reversible capacity of  $\sim 170 \text{ mAh g}^{-1}$  at a delithiation rate of 1 C, whereas a comparable graphite cell fabricated with a polyvinylidene fluoride (PVDF) binder failed to cycle.

Published by Elsevier B.V.

## 1. Introduction

Lithium-ion batteries (LIBs) that employ a layered transition metal oxide cathode, a graphite carbon anode, and a non-aqueous organic electrolyte containing  $\text{LiPF}_6$  salt in ethylene carbonate (EC)-based solvents are widely used as power sources in consumer electronics [1]. It is generally accepted that during the first cycle lithiation, electrolytes decompose to form a solid electrolyte interphase (SEI) film on the graphite anode [2]. SEI passivates the

graphite surface and prevents further solvent decomposition while allowing reversible lithium intercalation and de-intercalation between the electrolyte and the graphite anode.

Compared to EC, propylene carbonate (PC) is a more promising solvent because it offers good ionic conductivity and superior low-temperature performance. This is due to its low melting temperature of approximately  $-50^\circ\text{C}$ , which is far below that of EC ( $30^\circ\text{C}$ ). However, instead of forming an effective SEI, PC undergoes a detrimental decomposition process during cycling on graphite surfaces, causing exfoliation of the graphite and cell failure [3]. The introduction of additives to PC-based electrolytes was shown to form a desirable SEI layer on the graphite anode and considerably

\* Corresponding author. Tel.: +1 510 486 7207; fax: +1 510 486 7303.

E-mail addresses: [gliu@lbl.gov](mailto:gliu@lbl.gov), [gaolbnl@gmail.com](mailto:gaolbnl@gmail.com) (G. Liu).

improved battery performance [4]. Meantime, compared to EC-based electrolytes, addition of additives leads to a thinner SEI layer, smaller cell impedance, and better cell performance [5]. Vinylene carbonate (VC) has been proven to be an effective additive for LIBs [6,7], and a previous study indicates that the sacrificial decomposition of VC before carbonate solvents forms a stable SEI, which contributes to the improved cell performance [8]. Ouatani et al. performed XPS characterization to study the SEI structure on graphite anodes in VC-containing electrolytes, they used a synthesized polyVC as a reference compound, and polyVC was confirmed as the major component of the SEI [9,10]. A comprehensive investigation by Ota et al. also identified polyVC as the primary SEI component on graphite anodes, although other components, such as an oligomer of VC, a ring-opening polymer of VC, and polyacetylene were also identified in the SEI [11].

It remains a formidable challenge to develop a high-capacity battery system without sacrificing power, stability, safety and cost, a task requires optimizing the performance of every battery component [12]. In addition to other elemental battery parts, such as electrode active materials and electrolytes, a good binder is critical maintaining the electronic and mechanical integrity of battery electrodes [13], which directly relates to a stable cell capacity. In our research, we used chemically synthesized polyVC as a binder for fabricating graphite anodes. In an electrolyte with PC content as high as 30 wt%, the polyVC binder enhanced battery performance, with a reversible capacity of around 170 mAh g<sup>-1</sup>, at a delithiation rate of 1 C rate, whereas a comparable graphite cell fabricated with a PVDF binder an equivalent fabricated PVDF binder-based graphite cell failed to cycle.

## 2. Experimental

### 2.1. Materials

Vinylene carbonate was purchased from TCI America and passed through a basic Al<sub>2</sub>O<sub>3</sub> column to remove the stabilizer. All reagents were purchased from Sigma–Aldrich or TCI America and used without further purification. CGP-G8, purchased from ConocoPhillips, was used as the graphite anode. Battery-grade acetylene black (AB) was obtained from Denka Singapore Private Ltd, and PVDF KF1100 binder was acquired from Kureha, Japan. Electrolytes were purchased from Novolyte (now part of BASF), including 1 M LiPF<sub>6</sub> in EC and diethyl carbonate (DEC) (1/1 w/w), as well as 1 M LiPF<sub>6</sub> in PC. For our study, the electrolytes with different PC contents in this work were home-made using these two commercial electrolytes. 2325 coin cells were prepared using lithium metal as counter electrode.

**Synthesis of polyVC:** 5 g of purified vinylene carbonate (58 mmol) and 0.095 g (0.58 mmol) azobisisobutyronitrile (AIBN) were added into a 25 mL Schlenk flask. The reactants were degassed, without adding any solvent, by three cycles of freeze–pump–thaw before immersing the flask into an oil bath at 70 °C. After overnight reaction, the reactant was dissolved in dimethylformamide (DMF) and precipitated in diethyl ether. The powder product was recovered by suction filtration and vacuum dried at 60 °C for overnight. 3.8 g product was obtained with a yield of ~76%. <sup>1</sup>H NMR (500 MHz, DMSO-*d*<sub>6</sub>), δ 5.35 (t, 4H), <sup>13</sup>C NMR (500 MHz, DMSO-*d*<sub>6</sub>), δ 153.2, 76.2.

### 2.2. Characterization

A Bruker Biospin Advance II 500 MHz Nuclear Magnetic Resonance (NMR) spectrometer was used to collect the proton and carbon NMR spectra of the synthesized products. The polymer binder was coated on Cu foil for a Cyclic Voltammetry (CV) test. CV

and Electrochemical Impedance Spectroscopy (EIS) were conducted on a VMP galvanostat/potentiostat (Bio-Logic), while CV was characterized at a cycling rate of 0.1 mV s<sup>-1</sup>. The polyVC-based graphite electrode was prepared by coating a copper foil current collector with a slurry of CGP-G8 and polyVC in DMF. *N*-Methyl-2-pyrrolidone (NMP) was used as solvent in the slurry to prepare the PVDF-based graphite electrode. The electrodes were dried at 130 °C for 12 h in a vacuum oven. Slurry preparation, electrode coating, and cell fabrication were completed using standard techniques in the literature [14]. The loading of the graphite was controlled at ~3 mg cm<sup>-2</sup>. Lithium-ion cells were cycled for one cycle at a C/25 rate, lithiated for 12.5 h at a C/25 rate, and rested for 4 h before EIS measurement. The sample cells were brought to 10 mV before impedance measurement was taken at 0.01 Hz to 0.1 MHz.

Morphology of the electrode surface was characterized using a JSM-7500F scanning electron microscope (SEM). After cycling, the graphite electrodes were washed with dimethyl carbonate (DMC) solvent inside an argon-filled glove box to remove residual electrolyte. A homemade transfer system equipped with a gate valve and a magnetic manipulator was used for transfer of the highly sensitive samples from the pure argon atmosphere of the glove box to the SEM system.

## 3. Results and discussion

### 3.1. VC used as additive

VC has been shown to be an effective additive to suppress the exfoliation of graphite in PC [15]. Our study demonstrated a similar effect, as shown in Fig. 1(a). A graphite half cell using PVDF as a binder was cycled in 1 M LiPF<sub>6</sub> solution of PC with 2 wt% VC at a C/10 rate. Not only was graphite exfoliation prevented, the cell also showed a reversible capacity of ~260 mAh g<sup>-1</sup>. The cell efficiency kept improving and reached ~99% after the 24th cycle.

To further assess of the property of the SEI formed by VC-containing electrolytes, a graphite electrode with 10 wt% PVDF was used to assemble a coin cell using EC/DEC with 5 wt% VC. The cell was subsequently cycled for 10 cycles at a C/10 rate. It was then taken apart and the cycled electrode was re-used to assemble a new coin cell with a pure PC electrolyte. As shown in Fig. 1(b), this graphite electrode with pre-formed polyVC was able to tolerate PC for about 4 cycles at a C/10 rate, with a reversible capacity of ~280 mAh g<sup>-1</sup>. However, graphite exfoliation occurred at the 5th cycle. Two plausible explanations are proposed for this the cell failure: One possibility is that, because the graphite electrode was cycled for only 10 cycles in the sacrificial cell (using EC/DEC with 5 wt% VC), the SEI formation was not complete. Therefore, in the new cell with pure PC electrolyte, no further VC molecules existed for continuous repair of the SEI. Thus, initially, the graphite electrode with pre-formed polyVC was able to suppress the attack of PC molecule, but failed to do so after a few cycles. An alternative possibility is that, during the disassembly-reassembly process, the SEI on the electrode suffered from minor damage, which created a weak point sensitive to PC solvents. As a consequence, when re-used in the PC electrolytes it was unable to avoid exfoliation of the graphite.

### 3.2. PolyVC used as binder

In a prior investigation of lithium-ion electrode laminates as polymer composites, by Liu et al., a physical model was proposed in which the polymer binder forms fixed layers on the graphite particle surfaces [16]. The extra free polymer forms a conduction path where electrons are carried from the current collector through the whole electrode laminate. The active electrode material typically

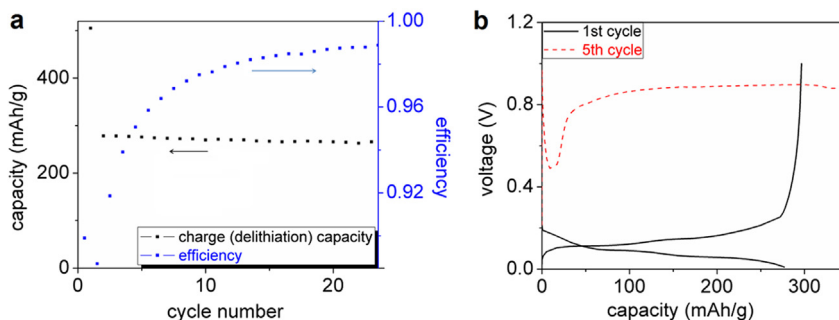


**Fig. 1.** Electrochemical performance of a graphite electrode with 10 wt% PVDF in (a) PC with 2 wt% VC at C/10 and (b) pure PC at C/10, the electrode was pre-cycled in a sacrificial cell in EC/DEC with 5 wt% VC for 10 cycles at a C/10 rate.

carries a functional chemical group from the production process [17,18], and the polymer binder tends to chemically bond or physically adsorb to the surface of the active material and form the fixed polymer layer [19,20]. This fixed polymer layer may change the surface property of the active material. Since polyVC is structurally similar to the VC-based SEI layer, the fixed polyVC layer is proposed to have the potential to facilitate SEI formation during cell cycling. PolyVC was synthesized via bulk free radical polymerization using AIBN [9,21], as shown in Fig. 2(b). The product was dissolved in DMF and precipitated in diethyl ether to remove any unreacted VC. The commercial VC normally contains butylated hydroxytoluene (BHT) in several parts per million. BHT is a radical scavenger, which is used to eliminate radicals and prevents undesirable polymerization of VC during storage and transportation. It is important to remove BHT since it will inhibit the radical reaction. Similarly, whenever the commercial VC is used as an additive, it is recommended that BHT be removed to make sure it does not interfere with the SEI formation from VC. A fractional vacuum distillation was performed to get rid of the BHT stabilizer in our study.

To assess the electrochemical stability of the polymer, CV of the PVDF and polyVC were performed in EC/DEC, as shown in Fig. 2(c) and (d). The working electrode was a copper foil coated with polyVC or PVDF film without graphite. A two-electrode coin cell was assembled using lithium foil as counter electrode for CV study. Electrolyte decomposition occurs with both polymers in the first cathodic scan, but no additional current flowed in the voltammogram in the following cycles. PVDF and polyVC should be

electrochemically stable as polymer binders for the negative electrode when lithium intercalation into graphite occurs below 0.2 vs.  $\text{Li}/\text{Li}^+$ . Furthermore, the peak corresponding to SEI formation in PVDF lasts from 0.9 V to 0.4 V (Fig. 2(c)), while such a signal is between 0.8 and 0.7 V for polyVC (Fig. 2(d)). It indicates that the electrolyte decomposition is more serious in PVDF compared to that in polyVC, since the intensity of this peak in PVDF is stronger than that in polyVC (as highlighted in Fig. 2(c) and (d)). When used in the cell, minor solvent decomposition leads to a thinner SEI with small impedance; this means that graphite-based lithium-ion cells should perform better with polyVC as their polymer binder.

The electrochemical performance of the lithium-ion cells based on PVDF and polyVC binder are shown in Fig. 3(a). All the cells were put in a formation process consisting two C/25 cycles and five C/10 cycles prior to 1 C rate. The performance at 1 C shows a clear advantage of polyVC binder. After an initial capacity drop, the capacities of the PVDF-based half cells increased and stabilized at  $70 \text{ mAh g}^{-1}$ , this capacity value from PVDF binder is low, due to the lack of conductive additives in the electrode. The polyVC-based cell, on the other hand, enabled a reversible capacity of  $\sim 250 \text{ mAh g}^{-1}$ . Fig. 3(b) shows the first cycle voltage curves of the graphite half cells based on these two binders, which are at a C/25 rate. Electrolyte decomposition at around 0.8 V enables the formation of SEI for both binders, but graphite reaches a higher capacity with polyVC binder even in the first cycle. The 75th cycle voltage curves in Fig. 3(c) indicate the large overpotential associated with the PVDF-

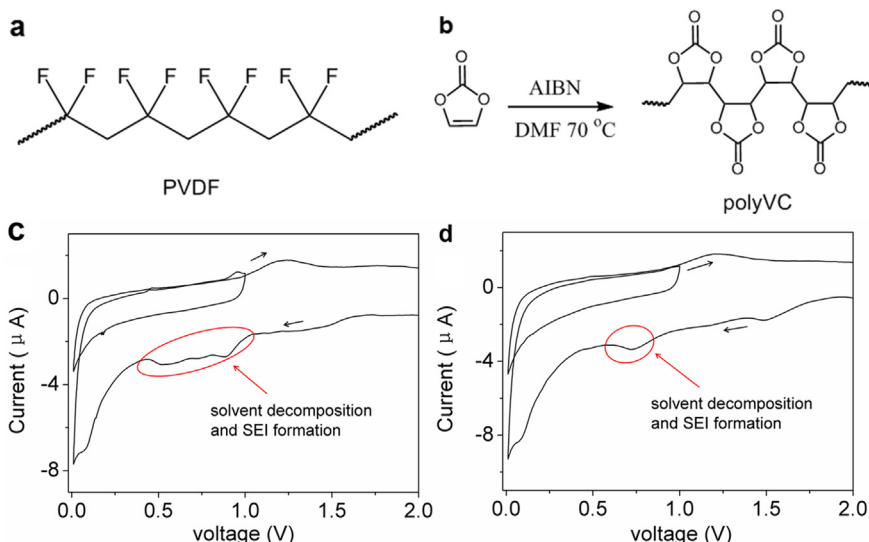


**Fig. 2.** (a) (b) Synthetic route, chemical structure and (c) (d) cyclic voltammetry of PVDF and polyVC binder, CV was tested in EC/DEC at  $0.1 \text{ mV s}^{-1}$ .

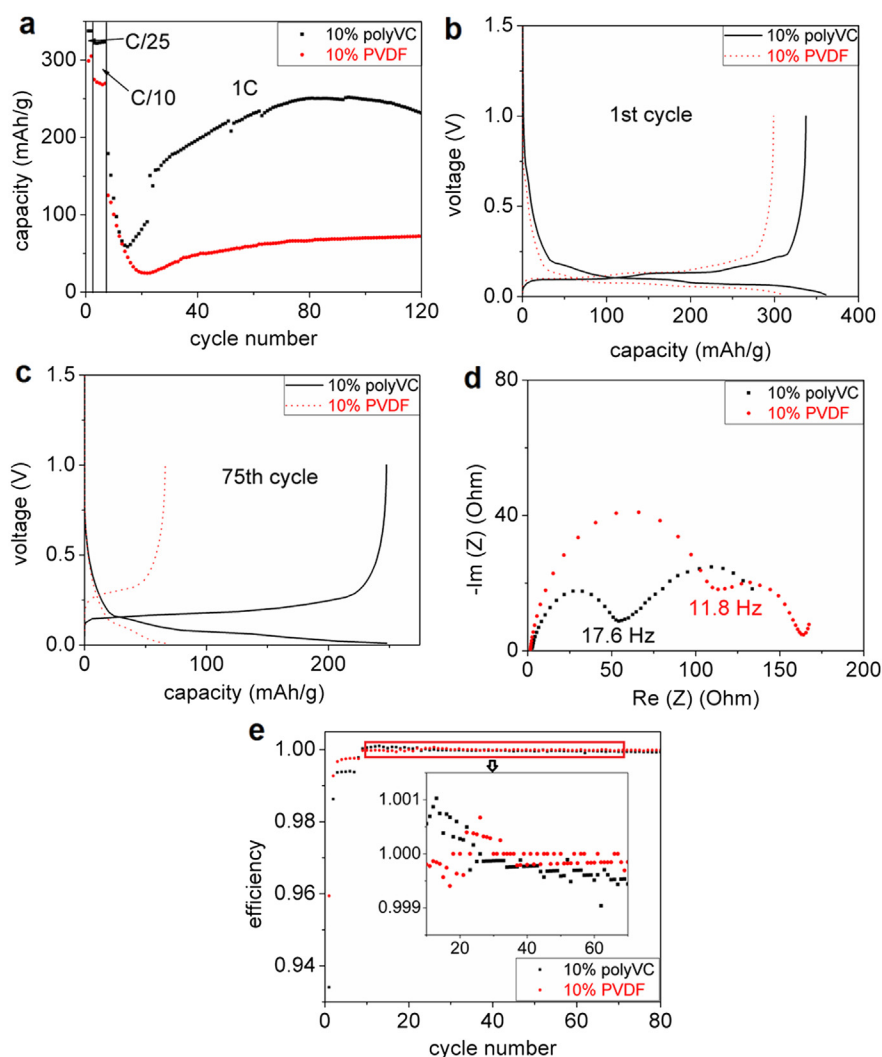


**Fig. 3.** (a) Charge (delithiation) capacities of graphite half cell based on 10 wt% polyVC and PVDF binder in EC/DEC at C/25 for 2 cycles, C/10 for 5 cycles and 1 C, (b) galvanostatic charge–discharge profiles of the two cells in the 1st cycle at a C/25 rate (c) galvanostatic charge–discharge profiles of the two cells in the 75th cycle at a 1 C rate, (d) electrochemical impedance, and (e) Coulombic efficiencies.

based cell, PVDF enabled a capacity of  $\sim 66.1 \text{ mAh g}^{-1}$ , while polyVC enabled a capacity of  $\sim 247.6 \text{ mAh g}^{-1}$ .

The impedance of the graphite half cells based on polyVC and PVDF is shown in Fig. 3(d). The sample cells initially went through a formation cycle at C/25, and the impedance was measured at half lithiation, since the voltage of the cell was relatively stable at that stage. The electron conduction of a half cell can be separated into two different ranges [22]. Long-range conduction describes the process where the electrons move from the current collector through the bulk electrode laminate, which is inversely proportional to the high frequency intercept of the impedance sweep. Typically, long-range conductivity is not a limiting parameter for the cell impedance. Short-range conduction describes the process where electrons move from the electrode into the electrolyte, which allows charge transfer at the electrode/electrolyte interface. This interface impedance, which normally also reflects the quality of the SEI, is the determining parameter for the cell impedance. Compared to that of PVDF, impedance was obviously smaller in the polyVC-based half cell, which further confirmed the information indicated in the voltage curves in Fig. 3(c). We propose that, because the polyVC-based graphite electrode induced less electrolyte decomposition, the

SEI in the cell exhibited smaller impedance than the PVDF-based cell. The impedance data are consistent with the CV data shown in Fig. 2(c) and (d), where the signal corresponding to solvent decomposition is more intense using PVDF than polyVC. Fig. 3(e) shows that the cells attain Coulombic efficiencies (CEs) as high as 99.95%.

Microscopic images of polyVC-based electrodes before and after cycling are shown in Fig. 4. The pristine electrode shown in Fig. 4(a) and (b) indicates an adequate porosity, which is calculated at  $\sim 48\%$ , and where the polymer binder is coated uniformly on the graphite particles. The morphology of the electrodes does not change much after one cycle in a half cell at a C/25 rate, and the porosity is also maintained well, which is important to facilitate lithium diffusion. Also, comparing Fig. 4(b) and (d) at higher magnification, the cycled active graphite particle surface in (d) does not show any obvious different compared to the pristine morphology in (b). This indicates that the SEI formed in the polyVC-based electrode is very thin, which is not visible in the electron microscope. A thin SEI is beneficial to obtain a good cycling performance [5], which is consistent with the data shown in Fig. 3. The morphologies of PVDF-based electrode are shown in Fig. 5. Because of the low polymer content in the laminate (10 wt%), it is difficult to



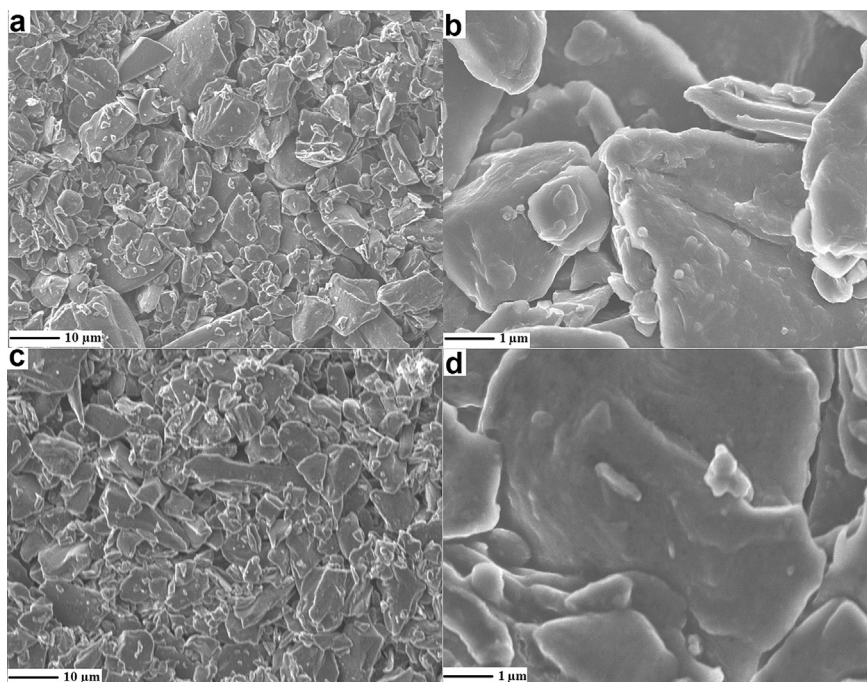


**Fig. 4.** SEM images of (a) (b) pristine electrode, (c) (d) electrode with 10% polyVC after 1 cycle in EC/DEC at C/25. The scale bars in (a) (c) are 10 μm and the scale bars in (b) (d) are 1 μm.

see the polymer under SEM either in pristine electrode (Fig. 5a and b) and cycled electrode (Fig. 5c and d).

The polyVC electrode binder performed well with the conventional EC/DEC electrolytes, and in light of the fact that VC additive prevents exfoliation of graphite electrodes in PC, we wanted to evaluate the performance of this new polyVC binder in a PC-containing electrolyte. Because PC is good ionic conducting

reagent with a low melting temperature, we hypothesized that, with addition of some PC into the traditional EC/DEC system, the low-temperature property would be largely improved. In this study, therefore, we gradually increased the PC content of the electrolyte. Fig. 6(a) shows cycling performance with a lithium counter electrode when the electrolyte was 20 wt% PC with 1 M LiPF<sub>6</sub>. When 10 wt% PVDF was used as binder, the graphite half cell

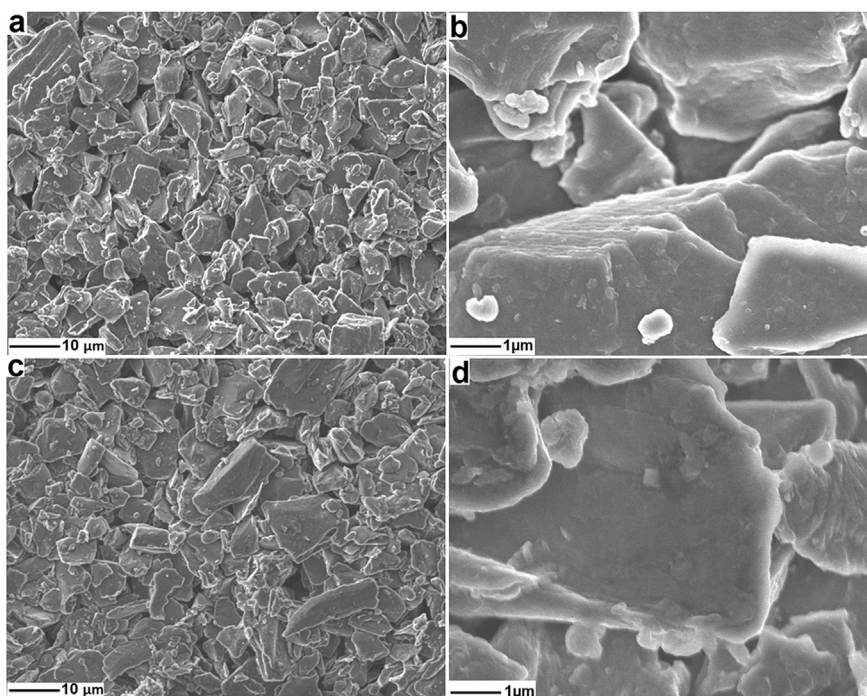


**Fig. 5.** SEM images of (a) (b) pristine electrode, (c) (d) electrode with 10% PVDF after 1 cycle in EC/DEC at C/25. The scale bars in (a) (c) are 10 μm and the scale bars in (b) (d) are 1 μm.

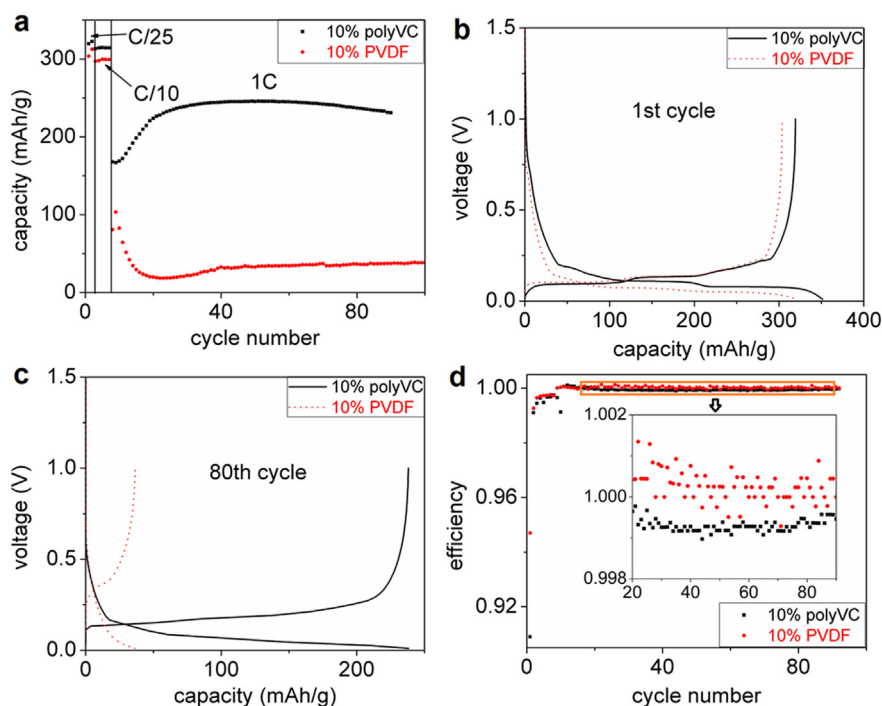


**Fig. 6.** (a) Charge (delithiation) capacities of graphite half cell based on 10 wt% polyVC and PVDF binder in electrolytes containing 20% PC at C/25 for 2 cycles, C/10 for 5 cycles and 1 C, (b) 1st cycle galvanostatic charge–discharge profiles at C/25 (c) 80th cycle galvanostatic charge–discharge profiles at 1 C and (d) Coulombic efficiencies.

only reached a capacity of around  $30 \text{ mAh g}^{-1}$ . With a stabilized capacity of  $\sim 250 \text{ mAh g}^{-1}$  at 1 C for 10 wt% polyVC, there was an obvious advantage for the polyVC binder. Neither PVDF nor polyVC show the influence by the 20 wt% PC in the first cycle voltage curves, as shown in Fig. 6(b). The 80th cycle voltage curves in Fig. 6(c) indicate a large overpotential associated with the PVDF-

based cell, at this point PVDF delivered a capacity of only  $31.2 \text{ mAh g}^{-1}$ , while polyVC delivered a capacity of  $238.1 \text{ mAh g}^{-1}$ , with CE of higher than 99.90%, as shown in Fig. 6(d).

With 30 wt% PC in the electrolyte, the capacity of the 10 wt% polyVC-based graphite half cell dropped because of the increased PC content, but still showed a good reversible capacity of

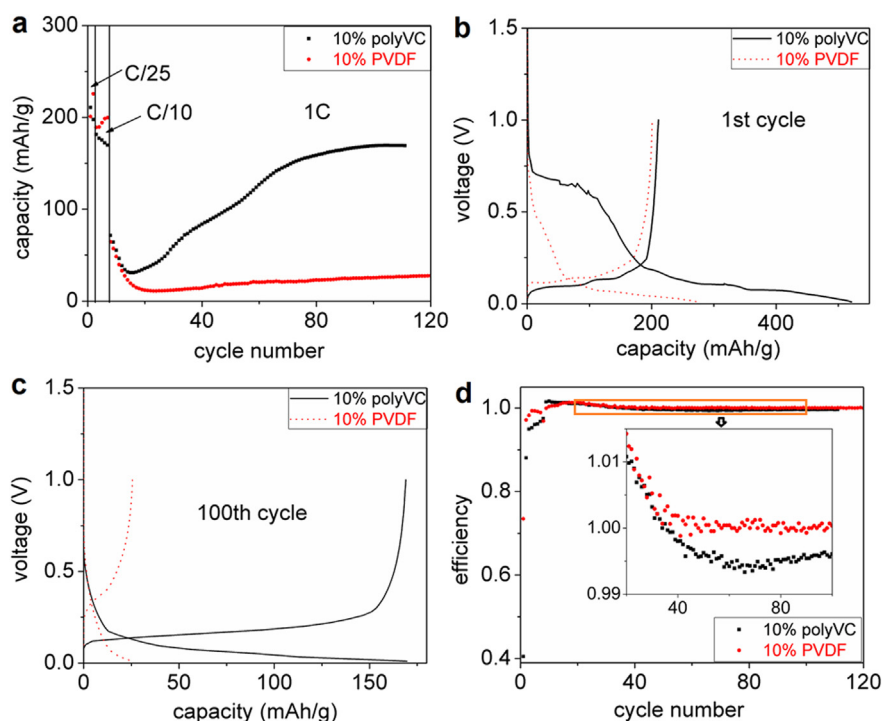


**Fig. 7.** (a) Charge (delithiation) capacities of graphite half cell based on 10 wt% polyVC or PVDF binder in electrolytes containing 30% PC at C/25 for 2 cycles, C/10 for 5 cycles and 1 C, (b) 1st cycle galvanostatic charge–discharge profiles at C/25 (c) galvanostatic charge–discharge profiles at the 100th cycle at a 1 C rate and (d) Coulombic efficiencies.

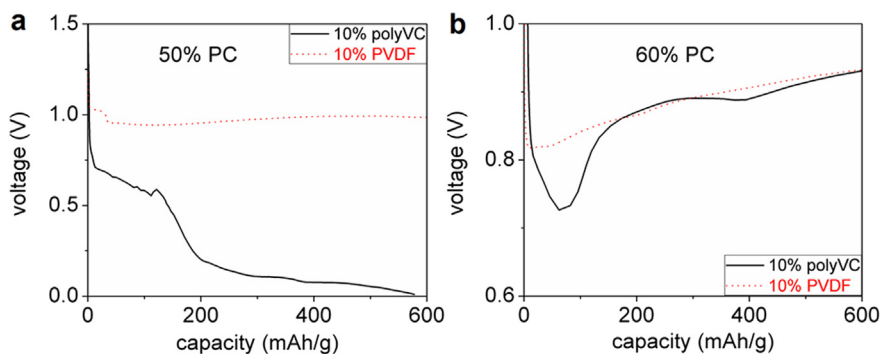


Fig. 8. Galvanostatic charge–discharge profiles of graphite half cells for (a) 50 wt% PC and (b) 60 wt% PC, based on 10% polyVC or PVDF, at C/25.

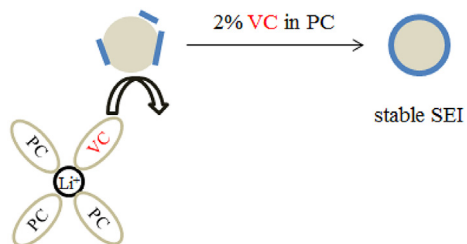
$\sim 170 \text{ mAh g}^{-1}$ . The 10 wt% PVDF-based graphite half cell only showed a capacity of  $\sim 25 \text{ mAh g}^{-1}$ . Although in this case the polyVC cells performed better than those with PVDF, this advantage is not apparent in the first cycle voltage curves, as shown in Fig. 7(b). The cell with PVDF binder barely shows a PC-related effect, while the performance of the polyVC-based cell indicates a

clear competition between exfoliation by PC and SEI formation by EC. A voltage plateau corresponding to this competition process occurs before lithium intercalation. The 100th cycle voltage curves in Fig. 7(c) indicate a large overpotential associated with the PVDF-based cell, at this point PVDF delivered a capacity of only  $26.2 \text{ mAh g}^{-1}$ , while polyVC delivered a capacity of  $162.1 \text{ mAh g}^{-1}$ .

Table 1

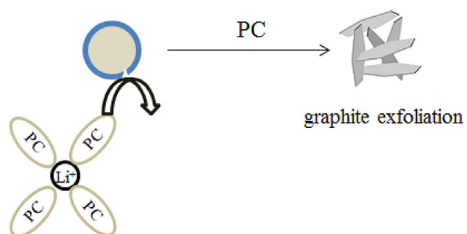
Schematics of the three different cases investigated in this work.

VC used as additive with PVDF binder



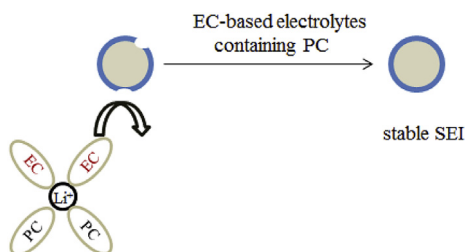
Exfoliation prevented, graphite shows reversible lithium intercalation and deintercalation

Electro-polymerized VC then re-use in PC, with PVDF binder



Reversible cycling initially, then exfoliation occurs

PolyVC used as binder



Protective polymer coating formed by polyVC binder further improved by EC

When the PC contents are as high as 50%, the 1st cycle voltage profiles are shown in Fig. 8(a). Graphite half cell with 10% PVDF was not able to tolerate this high amount of PC in the electrolyte. The voltage curve shows a long plateau at about 0.9 V, which corresponds to the decomposition of PC and exfoliation of the graphite anode. As for the polyVC-based half cell, after a voltage plateau at 0.7 V spanned for  $\sim 170 \text{ mAh g}^{-1}$ , the lithium eventually intercalates into the graphite. It implies that there is a competition between exfoliation of graphite by PC and SEI formation by EC, while EC decomposition seems to be dominant in the end, and the graphite surface is successfully passivated by stable SEI, which allows the cells to cycle reversibly.

When the PC content was increased to 60 wt% (Fig. 8b), neither PVDF nor polyVC-based graphite electrodes were able to prevent graphite exfoliation. Both PVDF and polyVC-based cells show exfoliation plateaus at around 0.85 V when cycled at a C/25 rate, which correspond to the continuous PC decomposition on the graphite surface. Further increase of the PC content resulted in graphite exfoliation for both polyVC and PVDF (data not shown).

Table 1 summarizes the three different cases investigated in this work. When VC is used as an electrolyte additive, the continuous improvement of the SEI formed by VC helps prevent graphite exfoliation caused by PC. When the graphite electrode was pre-cycled in a sacrificial cell with the VC-containing electrolytes, a polyVC formed *in-situ* enables lithium intercalation and deintercalation for the first several cycles; however, any defects in the SEI are sensitive to the pure PC electrolyte in the new cell, and finally exfoliation occurs. When used as electrode binder, polyVC facilitates the formation of a stable SEI, and lithium-ion cells based on polyVC show improved performance in electrolytes with different PC contents. To avoid the effects of conductive additives and to facilitate data analysis, we only used binder and active material (graphite) to assemble the electrode. Future studies may show that performance of polyVC-based lithium-ion cell could be further improved by addition of conductive additives.

The results in this study should inform the design of polymer binders for LIBs. The properties of polymer binders and electrolytes can be combined to produce a favorable environment at the electrode/electrolyte interface, which leads to an excellent cell performance. We propose that design of polymer binders should take into consideration of their behavior in a real lithium-ion cell. For example, once the electrode is assembled into a lithium-ion cell and begins to cycle, the polymer binder is swelled by the electrolytes and voltage is applied. This is a much different chemical and electrochemical environment than that of the electrode in a dry state. A successful binder design should take these factors into account.

#### 4. Conclusions

A binder is situated next to the active materials surface to provide mechanical properties for the electrode. However, as we demonstrate in this work, binders may also play a multifunctional role in lithium-ion battery electrodes. The search for an ideal binder seeks one that not only glues active materials together but also enhances battery performance. PolyVC, the major SEI component formed by VC-containing electrolytes, has proven to be a promising

binder for graphite anode in LIBs. PolyVC not only shows mechanical properties that are as good as those of the state-of-art PVDF binder, it also provides interface stability in a PC-containing electrolyte. Graphite half cells based on polyVC delivered a reversible capacity of  $\sim 250 \text{ mAh g}^{-1}$  at 1 C in EC-based electrolytes, compared to the capacity of  $\sim 70 \text{ mAh g}^{-1}$  using PVDF. With a PC content as high as 30 wt% in the electrolyte, polyVC-based cells were able to deliver a capacity of  $\sim 170 \text{ mAh g}^{-1}$  at 1 C, while the cells based on PVDF failed to cycle. This new binder, inspired by a performance-enhancing electrolyte additive, could potentially address the undesirable low-temperature performance of the state-of-art LIBs.

#### Acknowledgments

This work is funded by the Assistant Secretary for Energy Efficiency, Vehicle Technologies Office of the U.S. Department of Energy, under the Batteries for Advanced Transportation Technologies (BATT) and Applied Battery Research (ABR) Program. NMR measurements were performed at the Molecular Foundry. Electron microscopy experiments were conducted at the National Center for Electron Microscopy (NCEM). The two facilities are located at Lawrence Berkeley National Laboratory (LBNL), and are supported by the Director, Office of Science, Office of Basic Energy Sciences, of the US Department of Energy under contract no. DE-AC02-05CH11231.

#### References

- [1] J.B. Goodenough, Y. Kim, *Chem. Mater.* 22 (2009) 587–603.
- [2] R. Fong, U. von Sacken, J.R. Dahn, *J. Electrochem. Soc.* 137 (1990) 2009–2013.
- [3] H. Zhao, S.-J. Park, F. Shi, Y. Fu, V. Battaglia, P.N. Ross, G. Liu, *J. Electrochem. Soc.* 161 (2014) A194–A200.
- [4] K. Xu, *Chem. Rev.* 104 (2004) 4303–4418.
- [5] A.V. Cresce, S.M. Russell, D.R. Baker, K.J. Gaskell, K. Xu, *Nano Lett.* 14 (2014) 1405–1412.
- [6] Y. Wang, P.B. Balbuena, *J. Phys. Chem. B* 106 (2002) 4486–4495.
- [7] K. Ushirogata, K. Sodeyama, Y. Okuno, Y. Tateyama, *J. Am. Chem. Soc.* 135 (2013) 11967–11974.
- [8] Y. Wang, S. Nakamura, K. Tasaki, P.B. Balbuena, *J. Am. Chem. Soc.* 124 (2002) 4408–4421.
- [9] L. El Ouatani, R. Dedryvère, C. Siret, P. Biensan, S. Reynaud, P. Iratçabal, D. Gonbeau, *J. Electrochem. Soc.* 156 (2009) A103–A113.
- [10] L. El Ouatani, R. Dedryvère, C. Siret, P. Biensan, D. Gonbeau, *J. Electrochem. Soc.* 156 (2009) A468–A477.
- [11] H. Ota, Y. Sakata, A. Inoue, S. Yamaguchi, *J. Electrochem. Soc.* 151 (2004) A1659–A1669.
- [12] M. Armand, J.-M. Tarascon, *Nature* 451 (2008) 652–657.
- [13] M. Ling, J. Qiu, S. Li, H. Zhao, G. Liu, S. Zhang, *J. Mater. Chem. A* 1 (2013) 11543–11547.
- [14] G. Liu, H. Zheng, A.S. Simens, A.M. Minor, X. Song, V.S. Battaglia, *J. Electrochem. Soc.* 154 (2007) A1129–A1134.
- [15] X. Zhang, R. Kostecki, T.J. Richardson, J.K. Pugh, P.N. Ross, *J. Electrochem. Soc.* 148 (2001) A1341–A1345.
- [16] G. Liu, H. Zheng, X. Song, V.S. Battaglia, *J. Electrochem. Soc.* 159 (2012) A214–A221.
- [17] J. Qin, H. Zhao, R. Zhu, X. Zhang, Y. Gu, *J. Appl. Polym. Sci.* 104 (2007) 3530–3538.
- [18] J. Qin, H. Zhao, X. Liu, X. Zhang, Y. Gu, *Polymer* 48 (2007) 3379–3383.
- [19] J. Feng, J. Li, C.-M. Chan, *J. Appl. Polym. Sci.* 85 (2002) 358–365.
- [20] H. Hu, W. Yuan, H. Zhao, G.L. Baker, *J. Polym. Sci. Part A Polym. Chem.* 52 (2014) 121–127.
- [21] L. Ding, Y. Li, Y. Li, Y. Liang, J. Huang, *Eur. Polym. J.* 37 (2001) 2453–2459.
- [22] E. Pollak, G. Salitra, V. Baranchugov, D. Aurbach, *J. Phys. Chem. B* 111 (2007) 11437–11444.